Relaxation Studies on Power Equipment

S. Birlasekaran
School of Electrical & Electronic Engineering
Nanyang Technological University
639798 Singapore

and Yu Xingzhou
Power Grid Ltd.
Somerset Road, Singapore 238164

ABSTRACT

This paper describes a method of studying and modeling the dielectric relaxation for stationary power apparatus in an interconnected network to get the necessary aging indicators. The polarization phenomenon was studied using Recovery Voltage (RVM) and Polarization Current (PCM) Measurements on individual power apparatus and on network with other connected apparatus. Because of dielectric absorption in composite insulation, all RVM responses showed a single peak response and the response was linear with charging voltage. PCM decreased monotonically with a sudden drop in the initial period and after 100 s, it decreased very slowly and the response was linear with charging voltage. The responses were analyzed by modeling the dielectric function as an exponential function and as two-time dependent fractional power law function to determine suitable aging parameters. Exponential function model was found to fit both responses to get an equivalent electrical circuit of the system. Interrelation of RVM and PCM was established in most of the cases. Predicted dielectric response function for generator was more linear with time than for transformers and cable. In the frequency plane, it was found to have distinct regions of relaxation spectrum. Studies indicated that the parameters of fit for RVM response with each charging period differed from all RVM responses.

Index Terms — **Polarization current, recovery voltage, dielectric relaxation, Network dielectric response, universal fractional power law, extended Debye law.**

1 INTRODUCTION

THE use of polarization and depolarization current measurement (PCM) and the recovery voltage method (RVM) may be significant ways to detect aging of the insulation of operating power apparatus in a non-destructive manner [1]. Other non-destructive techniques [2] such as time-domain dielectric spectroscopy, laser intensity modulation method and pulsed electro acoustic method are used for research and diagnosis of insulation degradation but these popular techniques have no practicality as engineering tools to manage the aging apparatus. A number of these space charge "dielectric response" measuring techniques have been reviewed by Ahmed [3]. On the other hand the RVM and PCM techniques can be applied in the field and could be non-invasive if suitable precautions can be taken. In these measurements, the relaxation of bound and trapped charges with their characteristic dipoles and time constants in the range of 10 s to 5000 s can be determined by measuring either recovery voltage (RVM) or polarization current (PCM). RVM is less noise-sensitive and is simple to set up on-site. The main drawbacks are that the wave shape is sensitive to leakage currents due to input impedance of measuring voltmeter, polluted terminations, splices, and length and electrical characteristics of the connecting cable. Furthermore, the test duration is long, in the order of 5 hours. The response of the recovery voltage depends critically on the duration of charging and the operating temperature. RVM is used to study the degradation of paper-oil or XLPE insulated cables, capacitors and transformers. The diagnosis is done by comparing the initial slope, the maximum of the return voltage and the time at which the maximum of the return voltage occurs in the complete spectrum of measurements: good correlation has been reported with moisture content [4]. PCM is a transient current measurement technique. It is simple, but current varies significantly and often in incomprehensible ways attributed to

Manuscript received on 21 August 2001, in final form 29 May 2003.

"history" in the initial polarization period. The order of current magnitude and the rate of change in current with time are different for different insulation systems. The accuracy of the measurements of current magnitudes and times is important for signal processing as it contains relaxation information. In PCM, the measured current due to polarization will be comparable to background noise, especially in a generating station. The advantage of PCM is that its test procedure is simple and the measurement duration is considerably shorter than RVM.

The interpretation of the measured results in both RVM and PCM is very difficult as the measured dielectric response contains much information pertaining to the interfacial and dipolar relaxation mechanisms. The processed data may indicate the trend of deterioration of the insulation which must be extracted. Typically, the extended Debye model [11] is interpreted by the parallel RC elements representing geometrical leakage current, polarization and defects relaxations. Mathematical description of the equation of polarization spectrum for RVM with "n" polarization capacitors has been reported in [5]. To get the unknown $2(n+1)$ parameters, $2(n+1)$ equations have to be solved. With 2 polarisation capacitors, parameters were determined for a 330/11 kV transformer using the derived equations. The predicted polarization spectrum's voltage maximum (Vr max) and the slope did not match well with the measurements. Recently, transformations of measured data from time to frequency domains, and vice versa were attempted [6] where the advantages and disadvantages of respective measurements and determination of dielectric response function from polarization and depolarization current measurements were presented. Samples from aged cables were tested with low frequency dielectric spectroscopy [7, 17] in a range from 1 mHz to 1 kHz, with 5 V input. Measured ϵ' proportional to polarization capacitance) and ϵ'' proportional to polarization conductance) were found to be a function of frequency. The relaxation band varied from 1 mHz to 10 Hz. Relation between the frequency and time domains was established, up to 10 Hz. The dielectric response function was estimated from the depolarization current measurement. To improve RVM technique, "Repeated Short Circuit" [8] method was developed to minimize the influence of unknown internal or external resistances. Signal processing with "Division Polarisation Spectrum" [9] was developed to identify water-treed cable without any previous signature.

The main objective of this study is to develop a condition-monitoring technique for stationary power system equipment in an interconnected network. As it is very costly to disconnect working plants off-line, specifically, the RVM and PCM measurements were carried out on individual and connected power apparatus, which are installed in a network of two generating plants. The aim is to investigate the relaxation response of these equipments in connected mode, which is the operational layout. Thus instrumentation was developed to achieve flexibility to set the desired ranges, to study the linearity or otherwise in their responses with minimum charge injection and maximum signal to noise ratio, and to obtain the maximum number of sampling points for improved analysis. To characterize the response, models were built using extended Debye (ED) [5,10] and universal fractional power law (UFPL) models [11]. Analytical equations were derived for the generalized ED and UFPL models. Furthermore, parameters of the models were determined to obtain the best fit between the measurements and the calculated responses. Correlation between RVM and PCM was studied. Interpretations of these measurements and the comparability of these procedures were discussed. Derived low frequency responses showed the range of relaxation spectrum of different apparatus. The analysis shows that the existing models have to be improved for network responses.

2 BASIC THEORY OF DIELECTRIC RELAXATION

When a dielectric material is polarized with an electric field, $E(t)$, the charges induced at the electrodes are given by the sum of an instantaneous free space contribution and the delayed dielectric polarisation, $P(t)$, as

$$D(t) = \epsilon_0 E(t) + P(t) \tag{1}$$

In general, the observed polarisation, $P(t)$ contains two parts [12]

$$P(t) = P_{rapid}(t) + P_{slow}(t) \tag{2}$$

To predict this polarisation behavior, the dielectric response function $f(t)$ of the dielectric medium to specified electrical perturbation should be evaluated using equation (3).

$$f(t) \equiv 0 \quad \forall t < 0 \quad \text{and} \quad \lim_{t \to \infty} f(t) = 0 \tag{3}$$

If the dielectric materials behave like linear systems at low voltages, the slow polarisation process can be defined by equation (4) as the sum of delta-function perturbation of strength $E(t)\,dt$.

$$P_{slow}(t) = \epsilon_0 \int_0^t f(\tau) E(t-\tau)\, d\tau \tag{4}$$

The rapid polarization process can be combined with the first term on the right hand side of equation (1) and can be rewritten as

$$\epsilon_0 \epsilon r E(t) = P_{rapid}(t) + \epsilon_0 E(t) \tag{5}$$

ϵ_r is the relative dielectric permittivity at power frequency. Using the assumptions in equations (2), (4) and

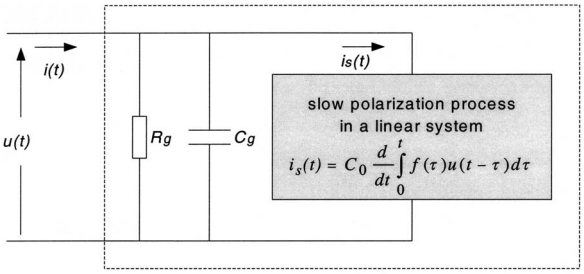

Figure 1. The model of a linear dielectric material.

(5), the current through the dielectric medium can be derived from equation (1) after substitution

$$j(t) = \sigma E(t) + \epsilon_0 \frac{d}{dt} \left\{ \epsilon_r E(t) + \int_0^t f(\tau) E(t-\tau) d\tau \right\} \quad (6)$$

If the dielectric material is considered as a homogenous one, equation (6) can be rewritten in terms of equivalent lumped parameters, as follows

$$i(t) = \frac{u(t)}{R_g} + \frac{d}{dt} \left\{ C_g u(t) + C_0 \int_0^t f(\tau) u(t-\tau) d\tau \right\} \quad (7)$$

In equation (7), $i(t)$ is the polarization current through the dielectric material and $u(t)$ is the applied voltage across the material. R_g represents the equivalent leakage insulation resistance, C_g represents the equivalent shunt insulation capacitance at operating frequency (50 Hz), and C_0 represents the equivalent geometrical capacitance in free space as shown in Figure 1.

2.1 MODELLING OF RELAXATION PROCESSES

2.1.1 EXTENDED DEBYE (ED) MODEL

The classical Debye model represents the "slow" polarisation process by a single element of a resistor and a capacitor in series [11]. However, the measured response function of power apparatus does not follow this exactly. As was shown by Jonscher [11], all experimentally observed behavior of composite dielectric materials can be represented by a number of exponents. If slow polarisation processes are represented by a number of relaxation time constants τ_i, the general dielectric response function

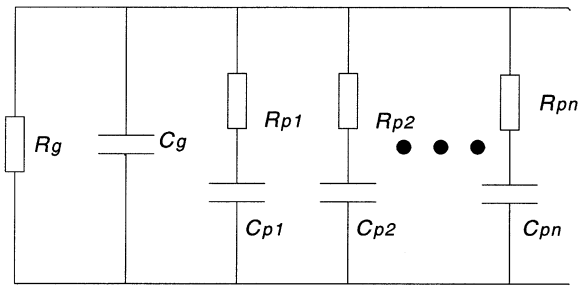

Figure 2. Extended Debye model.

can be written as

$$f(t) = \sum_{i=1}^{n} \frac{k_i}{\tau_i} \exp(-t/\tau_i) \quad (8)$$

Substituting this in equation (7), one can obtain the extended Debye model shown in Figure 2. This model consists of n relaxation elements.

2.1.2 UNIVERSAL FRACTIONAL POWER LAW (UFPL) MODEL

Furthermore, Jonscher [11] found that the response function in semiconductor and solid dielectric materials follow the universal fractional power law

$$f(t) = \frac{A}{(t/t_0)^n + (t/t_0)^m} \quad (9)$$

where $t_0 > 0$, $m > n > 0$, $m > 1$ and A is constant.

This dielectric response function had the following properties, indicating the dominance of fast and slow polarisation periods with respect to t_0

$$f(t) \propto (t/t_0)^{-n} \quad \text{for} \quad t \ll t_0 \quad (10)$$

$$f(t) \propto (t/t_0)^{-m} \quad \text{for} \quad t \gg t_0 \quad (11)$$

2.2 PREDICTION OF RVM RESPONSES BY USING ED MODEL

By using the ED model with n relaxation elements, the recovered voltage can be computed by using the proposed mathematical procedure presented herewith. Suppose all the capacitors are initially discharged, the dc voltage U_c is then applied across the test object for a charging period t_c (by closing S1 and opening S2 shown in Figure 3). The i-th capacitor C_{pi} will then be charged to a voltage U_{cpi}.

$$U_{cpi}(t_c) = U_c \left(1 - \exp\left(\frac{-t_c}{R_{pi} C_{pi}} \right) \right) \quad (12)$$

Then, the test object is short-circuited for t_d (by opening S1 and closing S2 of Figure 3), the remaining voltage U_{cpi} across C_{pi} is

$$U_{cpi}(t_c, t_d) = U_c \left(1 - \exp\left(\frac{-t_c}{R_{pi} C_{pi}} \right) \right) \exp\left(\frac{-t_d}{R_{pi} C_{pi}} \right) \quad (13)$$

For each pair of (t_c, t_d), the voltage across the i-th capacitor U_{cpi} (t_c,t_d) reaches a different value. For t_c/t_d = 2, the maximum value of U_{cpi} is achieved when $t_c = R_{pi}$ C_{pi} ln 3.

Now, as soon as the short circuit is removed (by opening S1 and S2 in Figure 3), the recovery voltage u_r is measured which will be due to the redistribution of all remaining charges in all the n polarisation capacitors and C_g. The ratio of the recovery voltage u_r to the voltage U_{cpi} across the i-th polarisation capacitor can be determined

from the equations derived from the equivalent circuit as

$$\frac{u_r(s)}{U_{cpi}(s)} = \frac{R_g C_{pi} s \prod_{j=1\cdots n}^{j\neq i} (R_{pj} C_{pj} s + 1)}{(R_g C_g s + 1) \prod_{j=1\cdots n} (R_{pj} C_{pj} s + 1) + \sum_{i=1}^{n} R_g C_{pi} s \prod_{j=1\cdots n}^{j\neq i} (R_{pj} C_{pj} s + 1)} = k_i \frac{s \prod_{j=1\cdots n}^{j\neq i} (s - z_j)}{\prod_{j=1\cdots n+1} (s - p_j)} \quad (14)$$

The total recovery voltage $u_r(t, t_c, t_d)$ is the sum of the individual contribution of remaining charges in each of the polarisation capacitors. This can be obtained for a given (t_c, t_d) pair by taking the Inverse Laplace transform of equation (14),

$$u_r(t, t_c, t_d) = \sum_{i=1}^{b} U_{cpi} \sum_{j=1}^{n+1} k_{ij} \exp(t \cdot p_j) \quad (15)$$

where

$$k_{ij} = k_i \frac{\prod_{y=1\cdots n}^{y\neq i} (s - z_y)}{\frac{d}{ds} \sum_{y=1\cdots n+1} (s - p_y)}\Big|_{s=p_j} \quad (16)$$

In this investigation, the prediction of the RVM responses was carried out using the derived expression (15) and a commercially available mathematical program MatLab [13]. This method of analysis was performed by considering 1 to 11 RC element-pairs, i.e. $n = 1$ to 11.

2.3 PREDICTION OF RVM RESPONSES BY USING UFPL MODEL

When the recovery voltage is measured under the open-circuit conditions, equation (7) can be rewritten by setting $i(t)$ to zero, i.e.

$$\begin{aligned} i(t) = \frac{u(t)}{R_g} + C_g \frac{d}{dt} u(t) + C_0 \frac{d}{dt} \int_0^{t_c} f(t-\tau) u(\tau) d\tau \\ + C_0 \frac{d}{dt} \int_{t_c}^{t_c + t_d} f(t-\tau) u(\tau) d\tau \\ + C_0 \frac{d}{dt} \int_{t_c + t_d}^{t} f(t-\tau) u(\tau) d\tau = 0 \\ \forall t > t_c + t_d \end{aligned} \quad (17)$$

During the charging period [0, t_c], $u(t)$ is constant and equal to U_c. $u(t)$ is zero during the discharging period [t_c, $t_c + t_d$].

$$\frac{d}{dt} \int_0^{t_c} f(t-\tau) u(\tau) d\tau = U_c (f(t) - f(t - t_c)) \quad (18)$$

and $$\frac{d}{dt} \int_{t_c}^{t_c + t_d} f(t-\tau) u(\tau) d\tau = 0 \quad (19)$$

Let $\beta = t - \tau$, then the last term on the RHS of equation (19) can be rewritten as

$$\begin{aligned} g &= C_0 \frac{d}{dt} \int_{t_c + t_d}^{t} f(t-\tau) u(\tau) d\tau \\ &= C_0 \frac{d}{dt} \int_0^{t - (t_c - t_d)} f(\beta) u(t-\beta) d\beta \\ &= C_0 \int_0^{t - (t_c + t_d)} f(\beta) \frac{d}{dt} u(t-\beta) d\beta \\ &\quad + C_0 f(t - t_c - t_d) u(t_c + t_d) \\ &= C_0 \int_0^{t - (t_c + t_d)} f(\beta) \frac{d}{dt} u(t-\beta) d\beta \end{aligned} \quad (20)$$

Assuming the response function $f(t)$ follows Universal Fractional Power Law, it tends to infinity when t tends to zero, i.e.

$$\lim_{t \to 0} f(t) = \lim_{t \to 0} \frac{A}{(t/t_0)^n + (t/t_0)^m} = \infty \quad (21)$$

It is singular at $t = 0$. Power-law singularity can be integrated through a change of variables whereby the singularity is eliminated [14]. In this case, this is achieved through the substitution.

$$\beta = \alpha^{1-n} \quad (22)$$

It allows the integral g to be re-written as

$$g = \frac{C_0}{1-n} \int_0^{t - (t_c + t_d)} \frac{A t_0^n}{1 + \left(\frac{\beta}{t_0}\right)^{m-n}} \frac{d}{dt} u(t-\beta) d\beta^{1-n} \quad (23)$$

The singularity is now eliminated from the integrand. If the parameters R_g, C_g, $C_0^* A$, t_0, n and m are already

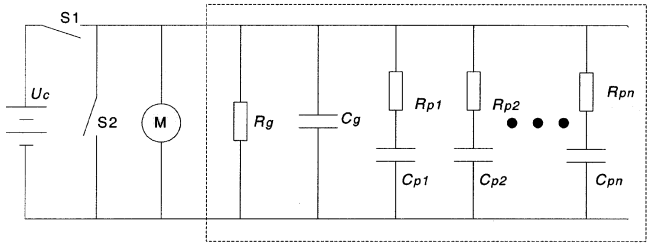

Figure 3. Layout for the prediction of RVM response using ED model.

known, the following algorithm can be used to calculate the recovery voltage. Now equation (17) may be written in the form

$$\frac{du(t)}{dt} + au(t) = g_0(t) + \Delta g(t,u(t)) = g(t, u(t)) \quad (24)$$

where $a = 1/R_g C_g \quad g_0(t) = U_c C_0/C_g(f(t-t_c) - f(t))$ (25)

and

$$\Delta g(t,u(t)) = \frac{C_0}{(n-1)C_g} \int_0^{t-(t_c+t_d)} \frac{At_0^n}{1+\left(\frac{\beta}{t_0}\right)^{m-n}} \frac{d}{dt} \times u(t-\beta)\, d\beta^{1-n} \quad (26)$$

Equation (24) has a solution

$$u(t) = \exp(-a(t-t_c-t_d)) \int_{t_c+t_d}^{t} \exp(a(\tau - t_c - t_d))\, g(\tau, u(\tau))\, d\tau \quad (27)$$

which may be solved by fixed-point iteration with the first term

$$u^1(t) = \exp(-a(t-t_c-t_d)) \int_{t_c+t_d}^{t} \exp(a(\tau - t_c - t_d))\, g_0(\tau)\, d\tau \quad (28)$$

and the higher terms being

$$u^n(t) = \exp(-a(t-t_c-t_d)) \int_{t_c+t_d}^{t} \exp(a(\tau - t_c - t_d))\, g(\tau, u^{n-1}(\tau))\, d\tau \quad (29)$$

3 EXPERIMENTAL PROCEDURE

3.1 RECOVERY VOLTAGE MEASUREMENT

The experimental procedure involved in the investigation follows the description given in Section 2.2 and others [10, 11, 15], using the measuring layout shown in Figure 4. Following the timing diagram shown, each recovered voltage across the test object can be recorded using the high impedance meter, M. By collecting the maximum value of $U_{r\max}$ and corresponding charging time t_c from each RVM curve, a polarization spectrum can be plotted ($U_{r\max}$ vs. t_c) to evaluate the peak recovery voltage. Two other important parameters of RVM curves are the time ($t_{\max}$) at which the peak occurs and the initial slope du_r/dt. Peak recovery voltage ($U_{r\max}$) with charging time (t_c) shifts to the small charging time with the increasing number of service years [10].

3.2 POLARISATION CURRENT MEASUREMENT

Polarization current measurement (PCM) is another method to estimate the insulating condition of dielectric material in the time domain [11]. The polarisation current through the test object is directly measured for an appropriate time after a constant voltage is applied to it. The initial current tends to be very large immediately after the application of constant voltage and it decays to extremely low value which is determined by the composite insulation characteristics of the power apparatus. The initial and the final slopes of the measured PCM response characterize the relaxation behavior in the apparatus.

3.3 TEST SITES FOR MEASUREMENT

Two power-generating companies at Singapore participated in the site testing. System "SYS1" is a 30 MVA emergency generator-transformer station while "SYS2" is a regular 300 MVA generating station with the schematic layout shown in Figure 5. Before starting any RVM and PCM test measurements, the generator busbar and other connecting terminals were cleaned, isolated with high impedance insulators if individual apparatus was studied, and all the connected auxiliary items such as the potential transformers and surge-suppressing capacitors were removed to minimize any chance of interference in the measurements. After the initial experience on the field, the actual RVM/PCM measurement was carried out on a clear day without much ambient disturbances.

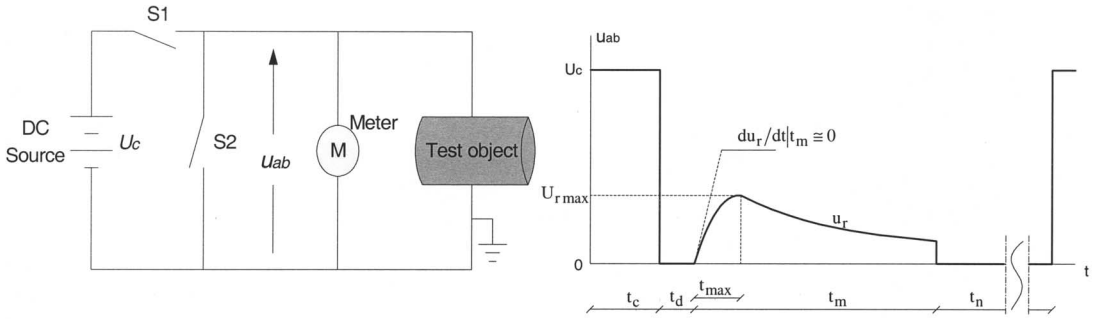

Figure 4. Layout and the timing diagram of an individual RVM.

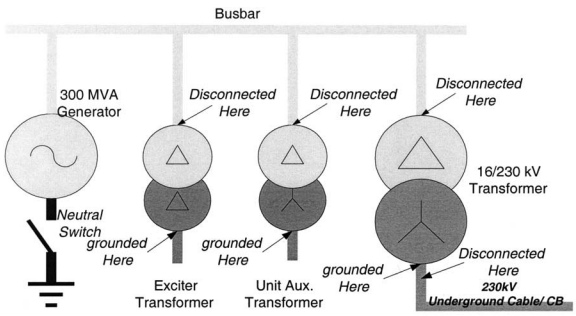

Figure 5. Generating system "SYS2" schematic diagram showing RVM/PCM test arrangements.

3.3.1 RVM AND PCM ON THE INDIVIDUAL APPARATUS

First, all the transformers were disconnected from the busbar. They were tested individually after isolation. The generator was tested with the busbar connected due to the difficulty of removing and re-connecting high current connections. As for the individual transformers and generator, the HV test lead was connected to the primary winding/stator terminals on the busbar side where the external three-phase terminals were shorted together. The windings on the other side were grounded through the transformer tank. The neutral point of the generator was isolated from the earth by opening the neutral switch. The underground single-core copper cables connecting the step-up transformer output to switchgear (CB) in "SYS1" and "SYS2" had oil-filled paper insulations. The cables were disconnected from the system at the external terminals of the step-up transformers as shown in Figure 5. The length of the cables under study were about 150 m each. The HV test lead was connected to the copper core of cables and its steel shield was connected to the grounded test lead.

3.3.2 RVM AND PCM ON THE OVERALL SYSTEM

To study the RVM and PCM behavior of the overall system, all the transformers were re-connected back to the generator busbar. The 3ϕ 16 kV-terminals of the busbar were shorted together. The HV test lead from the measuring system was connected to the busbar. After shorting other ends of 3ϕ 230 kV terminals of the transformers, they were grounded to the LV lead of the measuring system.

3.4 EXPERIMENTAL STUDIES FOR MODELLING

3.4.1 PARAMETERS CONTROLLING RVM STUDY

The recovery voltage is essentially dependent on the following parameters: the charging dc voltage U_c applied to the test object, the charging time t_c and the discharging time t_d. The first series of measurements was carried out in order to establish linearity in response so that the equipment relaxation behavior can be modeled irrespective of the charging voltage. The second series of measurements was done to evaluate the RVM responses of the transformers, generators and the cable as individual item of plant and the interconnected system with various charging times. The third series of measurements was done to understand the effects of charging and discharging time duration on the recovery voltage.

3.4.2 EFFECT OF APPLIED dc CHARGING VOLTAGE Uc

To develop a model for the dielectric response of the insulation system, the linearity in responses was evaluated. The perturbing applied dc voltage was not sustained at high voltage for long periods in order to prevent creation of any faults in the insulation due to dc voltage reversals and resulting adverse voltage stress distribution. Considering the voltage rating of developed measurement system, three different low dc voltages were selected to energize the test object. It was found that identical response was obtained by changing the polarity of the applied voltage. Typical measured response of transformer, Tb1 of "SYS2" is shown in Figure 6. The measured responses under three different U_c on each equipment were averaged and the results denoted as "Ref". "Ref" readings were then multiplied by the ratio of the applied voltages

Table 1. Comparison of the observed peak voltages $U_{r\max}$ with $t_{\max}$ of RVM responses. $t_c = 100$ s and $t_d = 50$ s at different U_c.

Power apparatus	$U_c = 50$ V		$U_c = 100$ V		$U_c = 150$ V	
	$U_{r\max}$	$t_{\max}$	$U_{r\max}$	$t_{\max}$	$U_{r\max}$	$t_{\max}$
Ta1 ("SYS1")-30 MVA	8.2 V	48 s	16.9 V	48 s	Out of range	Out of range
Tb1 ("SYS2")-300 MVA	7.9 V	67 s	15.6 V	66 s	23 V	66 s
Tb2 ("SYS2")-20 MVA	6.5 V	32 s	14.1 V	31 s	19.7 V	34 s
Tb3 ("SYS2")-2.17 MVA	5.3 V	28 s	10 V	28 s	15.1 V	28 s
Ga1 ("SYS1")-30 MVA	0.9 V	80 s	1.7 V	79 s	2.5 V	78 s
Gb1 ("SYS2")-300 MVA	1.2 V	101 s	2.3 V	106 s	3.4 V	102 s
Cb1a("SYS2")-220kV/300MVA	8.2 V	77 s	15.8 V	82.8 s	23.8 V	79 s
"SYS1"	1.8 V	82 s	3.6 V	84 s	5.2 V	86 s
"SYS2"	1.8 V	64 s	3.8 V	59 s	5.6 V	58 s

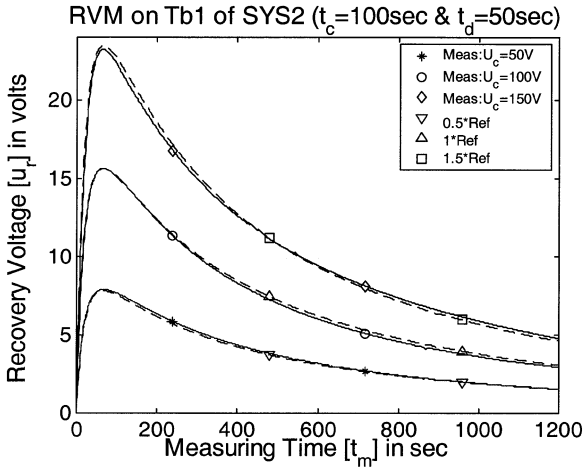

Figure 6. Effect of Applied Charging Voltage U_c on transformer, Tb1 of "SYS2".

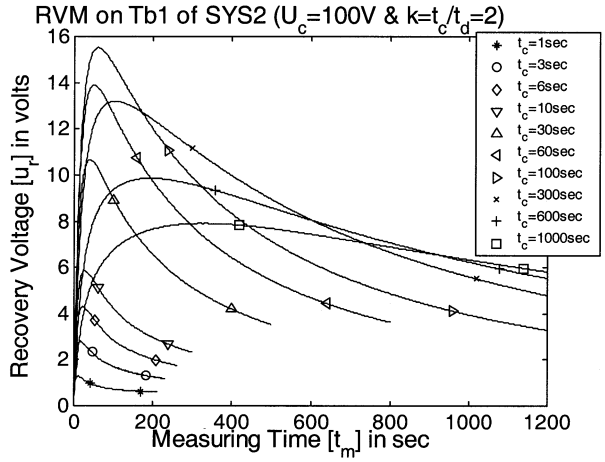

Figure 7. Effect of t_c by keeping $k = (t_c/t_d) = 2$ on transformer, Tb1 of "SYS2".

and compared with the measured ones. In all the studied cases, the two sets of curves fitted well thus indicating the linearity in responses with voltage either as an individual apparatus or as a system.

Table 1 lists the measured voltage peaks and the corresponding times to peak for a setting of $t_c = 100$ s and $t_d = 50$ s. The peak voltage $U_{r\max}$ and the time $t_{\max}$ at which it occurred varied between different equipments. Transformers and the cable had the maximum recovery voltage magnitudes and the individual generators the lower values. The inter-connected network system peak recovery voltage magnitude was higher than the individual generator peak value. Taking the response with U_c at 100 V for example, transformer Ta1 of "SYS1" had the highest $U_{r\max}$ of 16.9V at $t_{\max} = 48$ s and generator Ga1 of "SYS1" had the lowest $U_{r\max}$ of only 1.7 V at $t_{\max} = 79$ s. It implies that the relaxations of the composite insulation system within individual apparatus and overall systems might have different characteristics. It should be noted that for any apparatus, $t_{\max}$ was almost independent of U_c. The low $U_{r\max}$ of the generator may be due to its large geometrical capacitance. $t_{\max}$ varied irrespective of the rating of the apparatus.

3.4.3 EFFECT OF VARYING t_c AND t_d BUT AT CONSTANT K

To get the polarisation spectrum, the charging time t_c was systematically increased from a small initial value. The discharging time t_d was also increased, keeping the ratio $k = t_c/t_d$ at 2 for comparison purposes [10]. It is seen that RVM spectrum of all individual apparatus and systems had a standard response with a single peak [16] and our data also refutes this observation. Figure 7 shows the typical RVM responses of transformer, Tb1 of "SYS2". It can be seen that the responses with different charging times t_c were quite different. Those responses with short charging times, for example, $t_c < 10$ s, had a sudden rise and reached their peak very quickly. Then they stayed at a low value for $t_m > 800$ s. However, the responses after long charging times such as $t_c = 1000$ s had longer decay time. At the beginning of t_m, U_r rose slowly and after reaching the peak, it dropped marginally and still stayed with high value at their tails. Table 2 summarizes the three extracted quantities. The reported peak on each apparatus and system was the maximum value of all the measured RVM responses in that series of measurements connected with that apparatus or system. The peak magnitude and time of that occurrence varied for each apparatus.

The observation can be due to the following reasons. Taking Tb1 of "SYS2" in Figure 13 with short charging times of less than 100 s, only the relatively rapid parts (low time constants) of the slow polarisation processes were activated. They dominated the RVM response. During the discharging stage, some stored free charges will be depolarized over that short duration. At the measuring stage, these polarisations relaxed quickly and the confined charges were released very quickly and neutralized through the leakage resistance and geometrical capacitance of the insulation system. So the measured responses had a sharper shape. With long charging time greater than 600 s in Tb1, both rapid and slow parts of the slow polari-

Table 2. Measured $U_{r\max}$ at $U_C = 100$ V with the corresponding $t_{\max}$ and t_C .

Power apparatus	max ($U_{r\max}$)	$t_{\max}$	t_c
Ta1 ("SYS1")-30 MVA	18.8 V	49 s	30 s
Tb1 ("SYS2")-300 MVA	15.5 V	60 s	100 s
Tb2 ("SYS2")-20 MVA	15.1 V	38 s	60 s
Tb3 ("SYS2")-2.17 MVA	11.5 V	35 s	60 s
Ga1 ("SYS1")-30 MVA	2.2 V	90 s	6 s
Gb1 ("SYS2")-300 MVA	2.9 V	158 s	10 s
Cb1a ("SYS2")-220 kV / 300 MVA	17.8 V	62 s	30 s
"SYS1"	3.7 V	98 s	60 s
"SYS2"	4.1 V	77 s	60 s

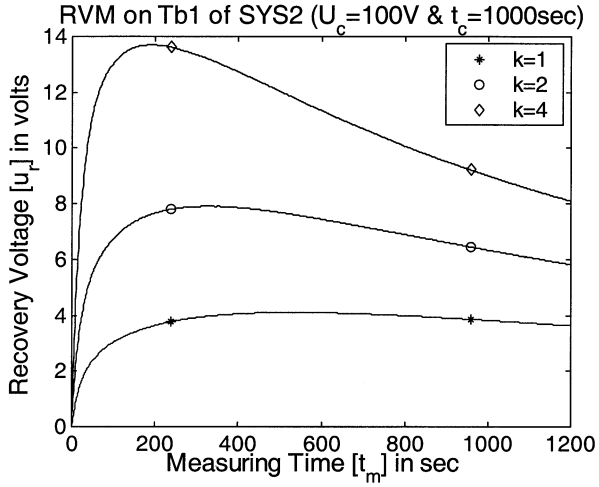

Figure 8. Effect of varying $k = t_c/t_d$ on transformer, Tb1 of "SYS2".

sation processes were activated. However the rapid polarisations with time constants less than the discharging period may have been over during the discharging stage. Only those very slow polarisations dominated the RVM behavior at the measuring stage. To relax completely, it would take a very long time. The trapped charges were released slowly so that the measured responses had a flatter shape. The magnitudes of the responses depended on the amount of remaining polarisation charges at that relaxation rate. The polarisation processes with different relaxation rates become dominant in turn on the measured responses for different t_c and t_d.

3.4.4 EFFECT OF VARYING k

In this study, t_c was fixed at 1000 s while t_d was set to 1000 s, 500 s and 250 s so that the corresponding ratios k were 1, 2, and 4 respectively. Figure 8 shows the typical results of the measured RVM responses. The magnitude of the recovery voltage increased with the ratio k in all equipment.

Table 3 lists $U_{r\max}$ and $t_{\max}$ of individual apparatus and interconnected systems by keeping U_c at 100 V, t_c at 1000 s and by varying t_d to obtain different values of k.

The numbers show that when $k = 1$ very slow polarised charges with time constants greater than 1000 s dominated the response behaviour. When $k = 2$, polarisation with time constants greater than 500 s contributes to the recovery voltage rise and fall characteristics. $U_{r\max}$ of 7.9 V was observed at $t_{\max}$ (t_m) of 336 s. Changing k from 1 to 2 increased the $U_{r\max}$ by 1.9 times and reduced the $t_{\max}$ by 0.66. With $k = 4$, polarisation with time constants greater than 250 s increased $U_{r\max}$ by 3.3 times to 13.7 V and reduced $t_{\max}$ by 0.38 times to 196 s. Table 2 showed $U_{r\max}$ was 15.5 V with $k = 2$ and $t_c = 100$ s indicating the dominant role of polarisation time constants greater than 50 s. With Gb1, the responses shifted to the right when the ratio k was increased. With $k = 4$, polarisation with time constants greater than 250 s increased $U_{r\max}$ by 4.6 times to 2.3 V and increased $t_{\max}$ by 1.53 times to 272 s. Table 2 showed $U_{r\max}$ was 2.9 V with $k = 2$ and $t_c = 10$ s indicating the dominant role of polarisation time constants greater than 5 s. Both of these observations confirm the role of the relatively fast polarisation process.

3.5 PARAMETERS CONTROLLING PCM STUDY

The objective of this PCM study was to evaluate the linearity of the dielectric response of the test object with U_c. In PCM study, three different dc voltages U_c were applied to the test object and the corresponding polarisation currents were measured. In practice, the polarisation current was measured about 1 s after the dc voltage application and the current can only be measured accurately for a limited duration [18].

3.5.1 FIELD MEASUREMENTS

PCM was done on all equipment and connected network. Typical result on transformer, Tb1 of "SYS2" is shown in Figure 9. All the measured current responses decayed monotonically with time and the computed resistance for Tb1 increased from 400 MΩ at 1 s to 1667 MΩ at 1000 s. PCM responses with $U_c = 50$ V, 100 V and 150 V are plotted in log-log scale to display clearly the characteristic slope variation at the initial and after critical changeover time. Similar to the RVM measurements, on each set of the readings, the measured responses under three different charging voltages U_c were averaged and labelled as "Ref". The measured responses are seen to

Table 3. Measured $U_{r\max}$ with tmax by varying k at $U_c = 100$ V and $t_c = 1000$ s.

	$k=1$		$k=2$		$k=4$	
Power apparatus	$U_{r\max}$	$t_{\max}$	$U_{r\max}$	$t_{\max}$	$U_{r\max}$	$t_{\max}$
Ta1 ("SYS1")-30 MVA	3.9 V	563 s	7.4 V	380 s	12.4V	275 s
Tb1 ("SYS2")-300 MVA	4.1 V	520 s	7.9 V	336 s	13.7V	196 s
Tb2 ("SYS2")-20 MVA	2.5 V	409 s	4.1 V	247 s	6.9 V	140 s
Tb3 ("SYS2")-2.17 MVA	4.1 V	264 s	7.1 V	205 s	10.1V	136 s
Ga1 ("SYS1")-30 MVA	0.8 V	302 s	1.3 V	222 s	2 V	184 s
Gb1 ("SYS2")-300 MVA	0.5 V	178 s	1 V	205 s	2.3 V	272 s
Cb1a ("SYS2")-220 kV/ 300 MVA	5.3 V	658 s	9.4 V	532 s	14.3V	371 s
"SYS1"	1.2 V	326 s	1.9 V	232 s	3.3 V	188 s
"SYS2"	0.7 V	164 s	1.5 V	133 s		

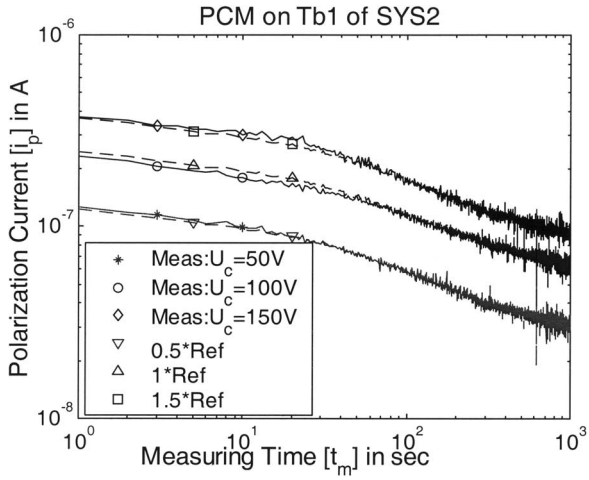

Figure 9. Effect of polarising voltage U_c on transformer, Tb1 of "SYS2".

match the "Ref" value when it is multiplied by the voltage ratios. The polarisation current on transformers and the cable decreased from 10^{-6} to 10^{-8} A and it dropped slightly during the initial period.

However, the polarisation current on the generators and the overall systems had higher values and it decreased from 10^{-5} A to 10^{-7} A. The computed resistance for Gb1 of "SYS2" varied from 12 MΩ at 1 s to 88 MΩ at 1000 s.

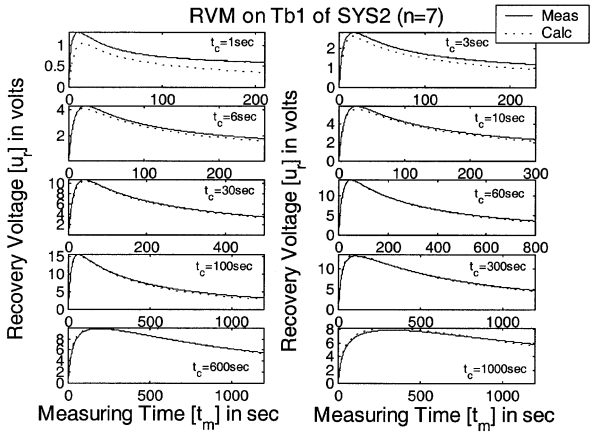

Figure 10. Measured and fitted RVM responses of transformer Tb1 for $n = 7$.

They had a sudden drop during the initial period that may be due to the charging of their large geometrical capacitance C_g. Table 4 lists the measured polarisation current values at the starting time t_m at 1 s and final time t_m at 1000 s.

At 1 s, the range of polarisation current for all apparatus with $U_c = 50$ V varied from 0.07 μA (714 MΩ) to 6.47 μA (7.7 MΩ) while at 1000 s, from 0.02 μA (2500 MΩ) to 0.69 μA (72.5 MΩ). The system response was linear when U_c was varied from 50 V to 150 V. All the individual apparatus had the unique two relaxation processes. Generator and cable had distinct fast and slow relaxation PCM characteristics.

4 ANALYSIS WITH RVM RESULTS

The measured results were analyzed with the Extended Debye (ED) and Universal Fractional Power Law (UFPL) Models.

4.1 FITTING WITH ED MODEL

The measured responses can be fitted to ED model with various relaxation elements and the quality of the fit can be evaluated. The objective was that the model should fit with every recovered voltage response obtained with a set of "t_c" and "t_d" in the entire measurement period. The various parameters in the model were determined using the developed algorithms to solve equation (15) and to get a minimum error between each measured result to the predicted response. The number of relaxation elements (n) was varied from 1 to 11 in our studies. The error in the curve fitting exercise was calculated using the formula

$$\text{Mean Relative Error (MRE)} = \frac{\sum_{1}^{Nc}\sum_{1}^{N_s}\left|\dfrac{Meas - Calc}{Meas}\right|}{N_{all}} \tag{30}$$

where N_c was the number of RVM responses, N_s was the number of sampled points in each RVM response and N_{all} was the total number of sampled points of all RVM re-

Table 4. Measured current at various polarising voltages. Polarisation current i_p at 1 s and 1000 s

	$U_c = 50$ V		$U_c = 100$ V		$U_c = 150$ V	
Power apparatus	i_p@1s	i_p@1000s	i_p@1s	i_p@1000s	i_p@1s	i_p@1000s
Ta1 ("SYS1")-30 MVA	0.19μA	0.03μA	0.36μA	0.05μA	0.56μA	0.08μA
Tb1 ("SYS2")-300 MVA	0.13μA	0.03μA	0.23μA	0.06μA	0.38μA	0.08μA
Tb2 ("SYS2")-20 MVA	0.12μA	0.04μA	0.27μA	0.08μA	0.38μA	0.12μA
Tb3 ("SYS2")-2.17 MVA	0.07μA	0.02μA	0.15μA	0.05μA	0.19μA	0.07μA
Ga1 ("SYS1")-30 MVA	6.47μA	0.39μA	Out of range	0.82μA	10.57μA	1.28μA
Gb1 ("SYS2")-300 MVA	4.25μA	0.57μA	Out of range	1.14μA	Out of range	1.71μA
Cb1a ("SYS2")-220kV/300MVA	0.52μA	0.04μA	1.04μA	0.09μA	1.54μA	0.13μA
"SYS1"	4.92μA	0.44μA	7.99μA	0.94μA	10μA	1.5μA
"SYS2"	4.76μA	0.69μA	Out of range	1.33μA	Out of range	1.95μA

Table 5. Fitted ED model parameters and its time constants for Tb1, Gb1 and Cb1a of "SYS2".

	Transformer, Tb1 Debye model ($n = 7$)		Generator, Gb1 Debye model ($n = 7$)		Cable, Cb1a Debye model ($n = 7$)	
R_g	1.88 GΩ	$t_g = 68$ s	0.33 GΩ	$t_g = 152$ s	1.36 GΩ	$t_g = 72$ s
C_g	36.3 nF		461 nF		53 nF	
R_{p1}	1.88 GΩ	$t_{p1} = 6.4$ s	0.13 GΩ	$t_{p1} = 0.8$ s	0.33 GΩ	$t_{p1} = 1.2$ s
C_{p1}	3.40 nF		5.96 nF		3.69 nF	
R_{p2}	1.81 GΩ	$t_{p2} = 44$ s	0.07 GΩ	$t_{p2} = 0.9$ s	0.32 GΩ	$t_{p2} = 8.3$ s
C_{p2}	24.5 nF		12.4 nF		26.1 nF	
R_{p3}	2.50 GΩ	$t_{p3} = 126$ s	0.13 GΩ	$t_{p3} = 4.3$ s	0.33 GΩ	$t_{p3} = 23$ s
C_{p3}	50.3 nF		33.1 nF		70.8 nF	
R_{p4}	11.4 GΩ	$t_{p4} = 149$ s	1.08 GΩ	$t_{p4} = 18$ s	4.34 GΩ	$t_{p4} = 31$ s
C_{p4}	13.1 nF		16.8 nF		7.1 nF	
R_{p5}	15.6 GΩ	$t_{p5} = 223$ s	0.86 GΩ	$t_{p5} = 39$ s	0.64 GΩ	$t_{p5} = 85$ s
C_{p5}	14.3 nF		44.7 nF		134 nF	
R_{p6}	5.74 GΩ	$t_{p6} = 230$ s	3.01 GΩ	$t_{p6} = 238$ s	2.19 GΩ	$t_{p6} = 228$ s
C_{p6}	40 nF		78.9 nF		104 nF	
R_{p7}	4.49 GΩ	$t_{p7} = 961$ s	5.91 GΩ	$t_{p7} = 6974$ s	2.21 GΩ	$t_{p6} = 984$ s
C_{p7}	214 nF		1180 nF		445 nF	
MRE		3.3%		8.9%		1.4%

sponses ($N_s \times N_c$). "Meas" represented the measured RVM response and "Calc" meant the calculated result by ED model.

4.1.1 RVM ON TRANSFORMER, Tb1

With reference to Transformer, Tb1 response fitting with $n = 1$, a match can be found only at $t_c = 60$ s. Increasing n to 3, a match is not found at $t_c = 1$ s. For $n = 7$, satisfactory fit can be observed in Figure 10. Similar satisfactory fitting was made on generator (Gb1), cable (Cb1a) with $n = 7$ or more elements.

4.1.2 ESTIMATED PARAMETERS FOR TRANSFORMER Tb1, GENERATOR Gb1 AND CABLE Cb1a OF " SYS2"

The calculated parameters of ED model and the associated time constants for the above fitting on individual apparatus are tabulated in Table 5 for the case n = 7.

Transformer, Tb1: R_g was around 1.9 GΩ, C_g was 36 nF and its t_g was 68 s for $n = 1$ to 11 elements. The range of polarisation time constants τ_{pi} varied from 6.4 s to 961 s. MRE decreased from 35% to 3.25% by changing n from 1 to 11.

Generator, Gb1: R_g was constant at 0.3 GΩ while C_g was around 465 nF. The range of polarisation time constants τ_{pi} varied from 0.8 s to 6974 s. MRE decreased from 51% to 8.8% by changing n from 1 to 11.

Cable, Cb1a: R_g was around 1.35 GΩ while C_g was around 53 nF. The range of polarisation time constants τ_{pi} varied from 1.2 s to 984 s. MRE decreased from 53% to 1.3% by changing n from 1 to 11

It was seen that R_g and C_g was constant for the variation of n. It was interesting to see that fitted R_g did not change much with other transformers also. But, C_g varied from 7.8 to 36 nF, which seemed to have some relation with their power capacity. For generators, C_g varied from 456 to 467 nF. For short length of cable, C_g was around 54 nF. The range of polarisation time constants varied widely with the increased number of relaxation elements (n). Time constants of polarisation elements for transformers and cable varied from 0.2 to 2000 s. For the generator, it varied between 0.4 to 35350 s. This trend confirmed the fact that the relaxations in real power apparatus had a range of time constants.

4.1.3 EXTRACTED AGING PARAMETERS

An analysis was made to find out how the ED model on transformer, generator and cable can be used to extract the following three ageing indicators: the maximum recovery voltage $U_{r\max}$, the time to peak $t_{\max}$ and the initial slope $d(u_r)/dt$. With $n = 7$, a satisfactory prediction could be made for Tb1, Gb1 and Cb1 and the typical result for Tb1 is shown in Figure 11. With Tb1, there were errors in

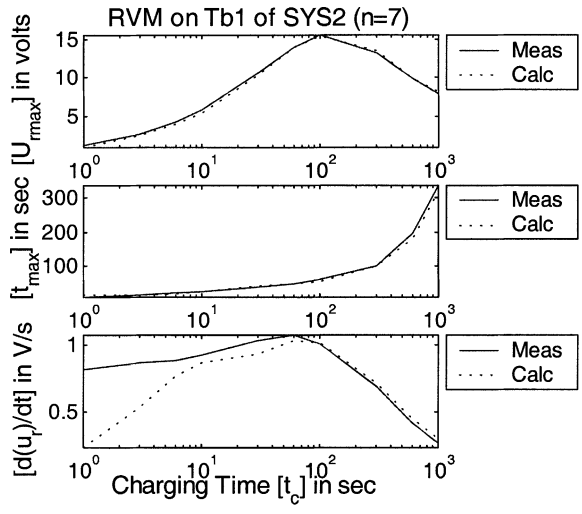

Figure 11. Measured and calculated $U_{r\max}$, $t_{\max}$ and initial slope of polarisation spectrum with ED model of 7 elements on transformer Tb1.

predicting initial slopes at short duration t_c and it could be due to measurement error.

4.1.4 FITTED PARAMETERS ON THE INDIVIDUAL RESPONSE

Since there was always some error in fitting the family of RVM responses of an apparatus with t_c, it was doubted that fitted parameters R_{pi} and C_{pi} may be a function of t_c. An analysis was made to estimate the extent of fitting reasonably with minimum number of elements say $n = 3$ on each curve obtained with t_c by using the converged values of R_g and C_g, and varying R_{pi} and C_{pi} for each t_c. The error for all individual fittings was kept at less than 1%. The conclusion was that there were deviations of R_{pi}, C_{pi} and τ_{pi}. The polarisation time constants τ_{pi} resulting from individual RVM curve fitting increased monotonically with the increased t_c in most of the cases. For the responses with shorter t_c, τ_{pi} resulting from individual curve fitting were usually lower than those τ_{pic} obtained by fitting all curves with single set of constant parameters. While for those responses with larger t_c, τ_{pi} had higher values than τ_{pic} in most of the cases. The time constants varied from 2 to 9000 s in the case of transformer, Tb1, 2 to 20,000 s in the case of generator, Gb1 and 2 to 1000 s in the case of cable, Cb1a.

Error (MRE) analysis was done to evaluate the quality of fitting due to parameters variation with t_c. The parameters obtained with $n = 3$ were used for the analysis. The error plot shown in Figure 12 with single curve fitting on

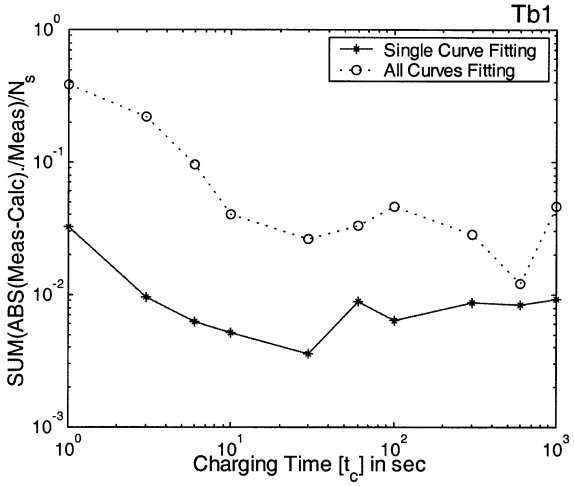

Figure 12. Comparison of MRE of each RVM response (t_c) fitting and all RVM responses "(t_c's)" fitting for transformer Tb1.

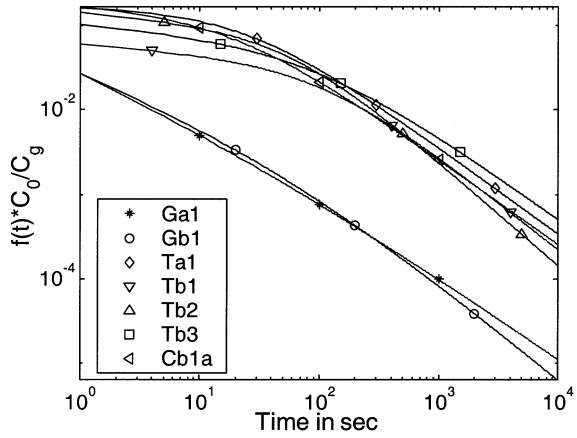

Figure 13. Fitted relaxation function $f(t)$ in UFPL model for generators, transformers and cable.

individual RVM response with one t_c was one order lower than the all curves fitting on RVM responses with the selected t_c. It suggests that the ED model has to be modified by taking into account the parameter variation with changing t_c.

4.2 FITTING WITH UFPL MODEL

The measured RVM responses can be fitted to UFPL model using the steps described in section 2.3. For the model, calculated R_g and C_g from ED model were used. Table 6 shows the determined parameters of the UFPL model on different power apparatus. The predicted dielectric response function of each individual apparatus is shown in Figure 13. The computed error of calculated results with reference to measured results after fitting to this model varied from 10% to 36% depending on the apparatus. The time t_0 dividing the ideal Debye behavior and the universal dipolar behavior varied from 19 s to 108 s. Universal dipolar response's fractional slope "n" varied from 0.04 to 0.62 while fractional slope 'm' varied from 1 to 1.22. Predicted dielectric response function of Generator was more linear in comparison with transformers and cable.

4.2.1 CALCULATED RVM RESPONSES FOR ALL " t_c"WITH UFPL MODEL PARAMETERS

The calculated RVM responses of tested equipment using the fitted UFPL model parameters for all "t_c" were

Table 6. Fitted UFPL model parameters for transformers, generators and cable.

	$R_g * C_g$	A* C_0/C_g	t_0	m	n	SUM $((i(t)/C_g)^2)$	MRE
Ta1	42.3	0.15	26	1.02	0.04	8.45	11%
Tb1	68.4	0.035	108	1.11	0.12	1.54	10%
Tb2	19	0.085	55	1.22	0.13	32.78	15 %
Tb3	19.1	0.056	94	1	0.14	67.83	36 %
Ga1	61.6	0.0041	31	1	0.62	0.75	30 %
Gb1	150.5	0.003	52	1.16	0.58	0.59	10 %
Cb1a	76.5	0.14	19	1	0.08	12.23	23 %

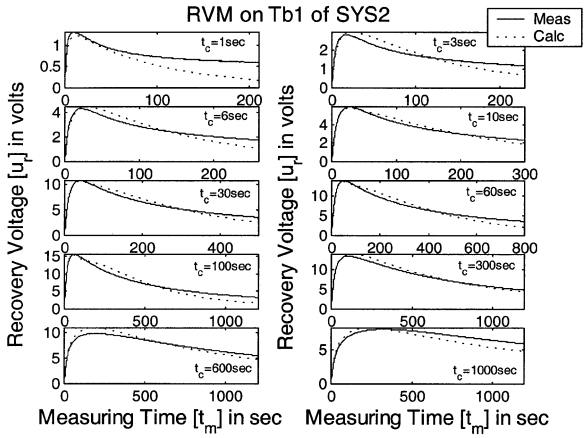

Figure 14. Measured and calculated RVM responses for transformer Tb1.

compared with the measured results. Typical results on transformer, Tb1 are plotted in Figure 14. For t_c = 1 and 1000 s, calculated and measured responses did not fit well.

4.2.2 FITTED UFPL PARAMETERS ON THE INDIVIDUAL RVM RESPONSE

A very good fitting shown in Figure 15 on individual response was made by varying UFPL model parameters listed in Table 6. For individual response fitting, the parameters varied with "t_c". The calculated model parameters t_0 and $A * C_0 / C_g$ were less than the values shown in Table 6. m and n had to be changed for the range of "t_c" from 10 s to 100 s.

4.2.3 ERROR ANALYSIS

The calculated MRE on the predicted RVM responses using UFPL model is shown in Figure 16. A significant reduction in error is obtained with individual response—single curve fitting. This analysis also suggests that the model is to be modified by taking into account

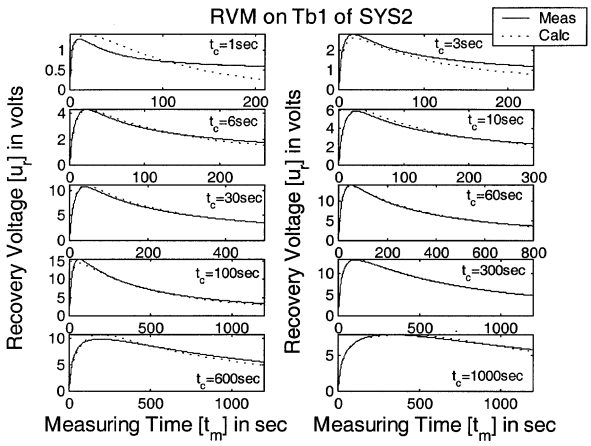

Figure 15. The measured and calculated RVM individual response for transformer Tb1.

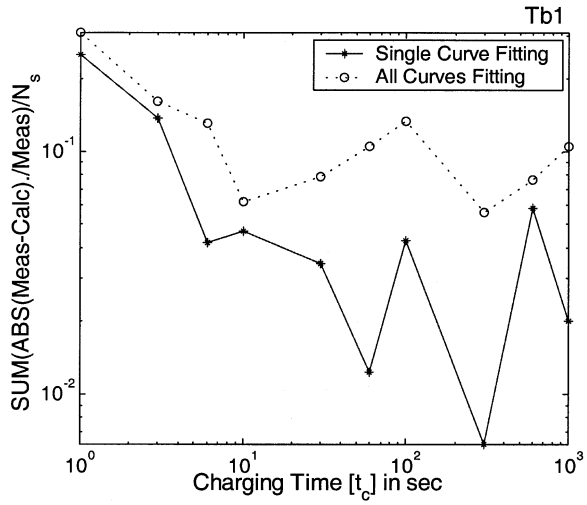

Figure 16. Variation of MRE on UFPL model.

the variation of the parameters with charging time t_c as shown in section 4.1.4.

5 ANALYSIS WITH PCM RESPONSES

Since the system response was linear with voltage on RVM and PCM, the validity of the models using RVM was verified with PCM.

5.1 FITTING WITH ED MODEL

Using ED model parameters on RVM, a comparison was made between calculated and measured currents. A close agreement was seen on polarization current measurements on transformers and cable. Typical result on transformer, Tb1 is shown in Figure 17. MRE on the fitted result with the measured one on Tb1, Cb1a and Gb1 were 5.2%, 1.8%, and 52% respectively. For generator, the fitting was not good.

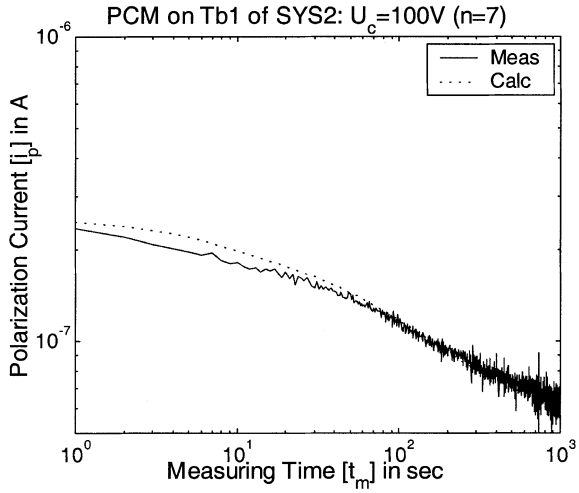

Figure 17. Measured and calculated PCM response using ED model parameters.

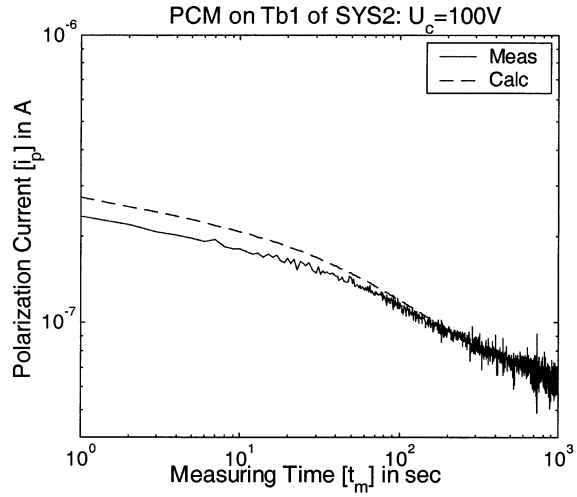

Figure 18. Measured and calculated PCM response using UFPL model parameters.

5.2 FITTING WITH UFPL MODEL

Using UFPL model parameters on RVM, polarization currents were predicted for all apparatus. Calculated current on transformer, Tb1 is shown as dotted line in Figure 18 with the measured results. MRE for Tb1 and Cb1a were 5% and 8.2% respectively. It was not possible to get a good fit with UFPL model on generator polarisation current measurements also. MRE was 73% with "Gb1".

6 ANALYSIS ON NETWORK RESPONSE

Network "SYS2" consisted of three transformers "Tb1", "Tb2", "Tb3", and a generator "Gb1". Measured RVM on network "SYS2" is shown as solid line in Figure 19. Since ED model parameters predicted RVM and PCM satisfactory, parameters on each apparatus was used for network prediction. Since ED model is a parallel-connected RC element, it could be extended easily to any number of connected apparatus in the network.

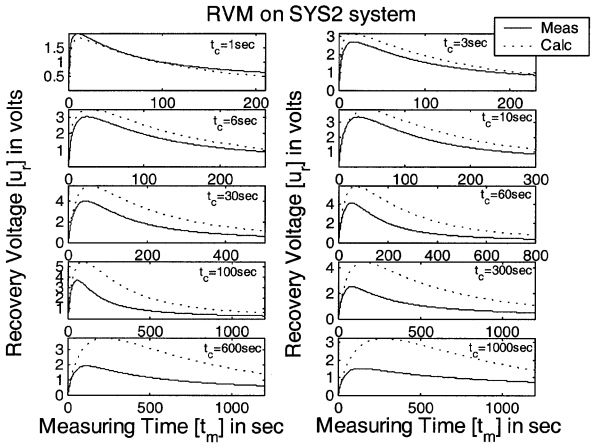

Figure 19. Measured and calculated RVM network response using ED model parameters.

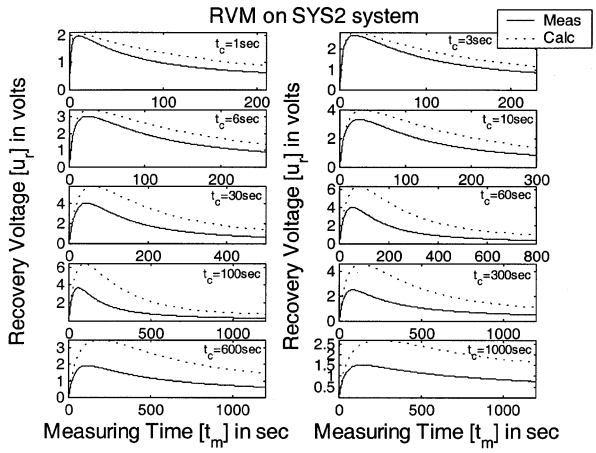

Figure 20. Measured and calculated RVM network response using individual ED model parameters.

6.1 COMPARISON OF NETWORK RESPONSE USING ED MODEL PARAMETERS

Since the number of network elements will increase significantly in ED model, the analysis was restricted with $n = 3$ on each apparatus of network "SYS2" consisting of three transformers and generator connected in parallel as shown in Figure 5. The calculated RVM with 14 elements in ED model in Figure 19 did not fit well with the measured response. It fitted only with "*tc*"= 1s. For a small network "SYS1", the fitting was good except with "*tc*"= 1 s.

6.2 COMPARISON OF NETWORK RESPONSE USING ED MODEL PARAMETERS ON INDIVIDUAL RESPONSE CURVE

The calculated RVM responses using the parameters on each "t_c" were compared with the networked RVM results. A better fit was obtained with "SYS1" network. But with "SYS2" network, the fit shown in Figure 20 was not good. The match was bad as "t_c" increased. The measured recovery voltage with long t_c was lower than the calculated recovery voltage. It clearly indicated that injected coulombs were lost during network measurement. It appeared that some charge might have dissipated locally in the relaxation elements and/or on the increased stray conductance during network measurement.

6.3 ERROR ANALYSIS

MRE of model with the measured results was computed. With "SYS1", MRE with individual response curve was one order down of the computed error on all response curves. In "SYS2", no remarkable MRE change was observed between single and all response curves fitting shown in Figure 21. MRE with ED network model

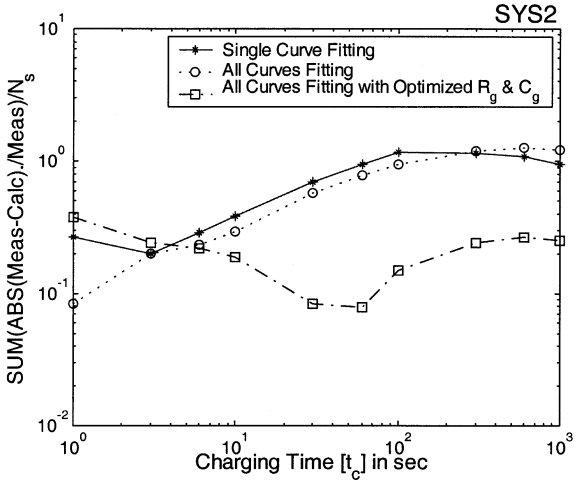

Figure 21. Comparison of MRE after optimizing R_g and C_g of network.

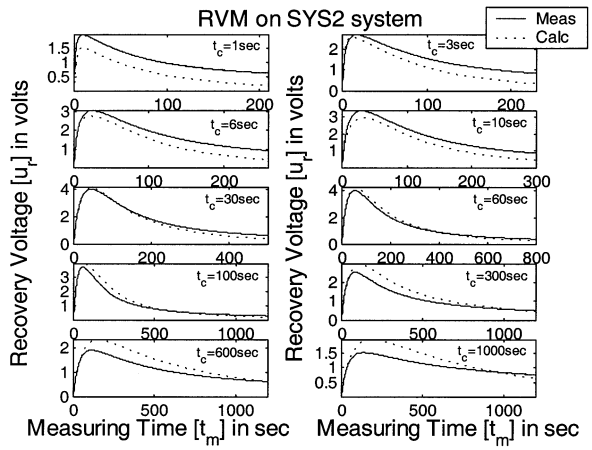

Figure 22. Measured and calculated RVM responses with optimized R_g and C_g.

parameters for "SYS1" and "SYS2" were 16% and 69% respectively.

Further analysis on the network responses was made by optimizing C_g and R_g to reach minimum MRE. After optimization of R_g and C_g of network "SYS1", the minimum error was 9%. In "SYS2", a significant improvement was achieved as shown in Figure 21 and MRE was brought down from 69% to 20%. The calculated RVM results for "SYS2" with the optimized parameters of R_g and C_g in ED model are shown in Figure 22. It appeared that ED model could be used for network prediction if parameters from individual curve fitting were used.

7 PREDICTION OF LOW FREQUENCY RESPONSE CHARACTERISTICS USING ED MODEL

Since the relaxation behaviour of power apparatus can be better understood in the frequency plane, the fitted

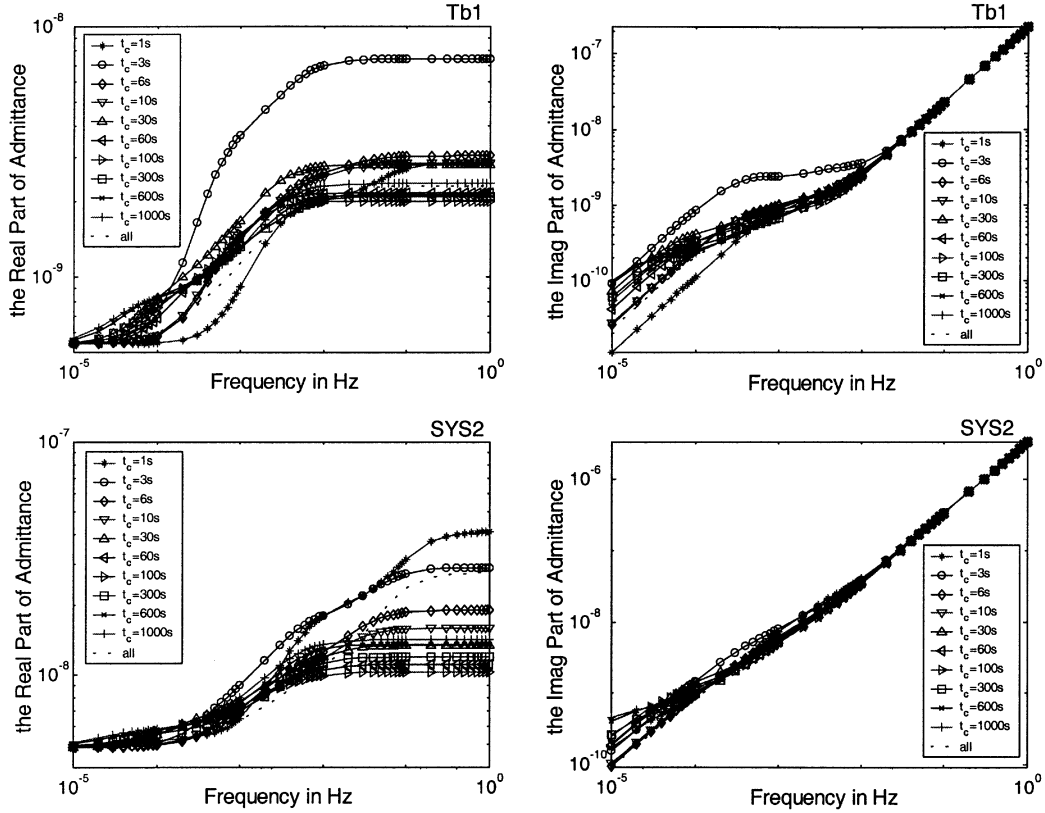

Figure 23. Variation of the real and imaginary parts of admittance using ED model.

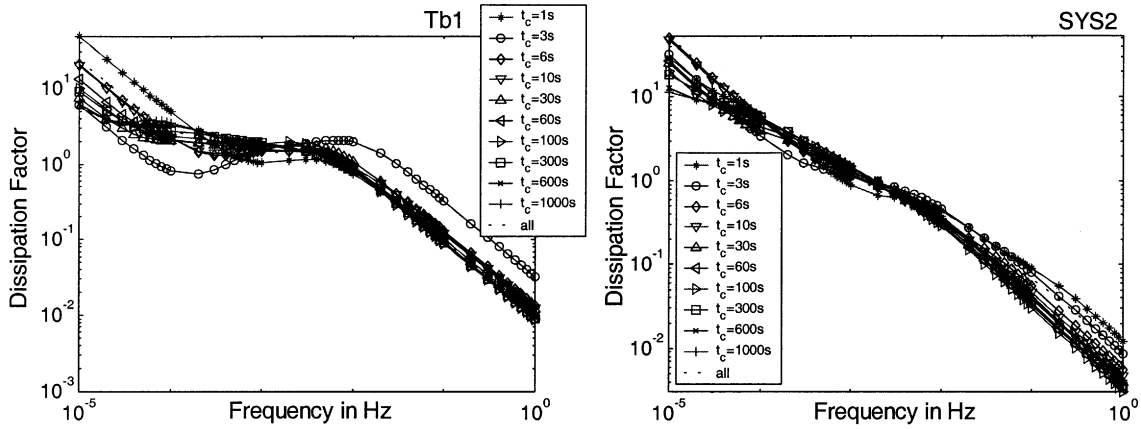

Figure 24. Variation of the dissipation factor using ED model.

ED model was used to identify the relaxation frequency ranges. The parameters of ED model derived from individual RVM response curve using three relaxation elements for an apparatus were used to predict the variation of real and imaginary parts of admittance and loss angle in the frequency plane. The computed response using parameters of all RVM response curves fitting was also plotted as dotted line.

7.1 VARIATION OF REAL PART OF ADMITTANCE

Figure 23 shows the computed low frequency response characteristics of transformer, Tb1 and network "SYS2". The LHS Figure 23 shows the variation of real part of admittance with frequency, and charging time "t_c". The RHS of Figure 23 shows the variation of imaginary part of the admittance with frequency, and charging time "t_c". The LHS figure shows three distinct frequency regions on the predicted real part of the admittance response. In the initial range, the magnitude of real part of admittance was small and it increased slowly. The frequency limits for transformers/cable and generators/networks were 10^{-4} Hz and 10^{-3} Hz respectively. This may be due to leakage resistance of the individual apparatus. In the second region, the real part of admittance increased appreciably due to relaxation elements. The frequency limits for transformers/cable and generators/networks were 20 mHz and 200 mHz respectively. In the last region, the admittance was maximum due to the contribution of various relaxation and leakage resistive elements. Hence, midregion represents the band of time constants of relaxation elements. The variation of admittance with "t_c" suggested the possibility of the existence of time/frequency dependent R and C relaxation parameters. As a network, the trend in "SYS1" and "SYS2" followed the respective generator responses Ga1 and Gb1 respectively.

7.2 VARIATION OF IMAGINARY PART OF ADMITTANCE

The RHS of Figure 23 shows two distinct regions on the imaginary part of admittance. In the first region, imaginary part of admittance increased slowly with frequency due to relaxation elements. Change in slope was due to the contribution of relaxation capacitors at different frequencies. The frequency limits for transformers/cable and generators/networks were 10^{-2} Hz and 10^{-4} Hz respectively. In the second region, it varied linearly with frequency like a single capacitor. Network response followed the generator response.

6.4 VARIATION OF DISSIPATION FACTOR (TAN δ)

Dissipation factor is a ratio of active current to reactive current if we assume a parallel RC configuration. The predicted tan δ in Figure 24 had three regions. In the first region, loss angle decreased with frequency. The frequency limits for transformers/cable and generators/networks were 2×10^{-4} Hz and 10^{-3} Hz, respectively. For transformer, in the second region it remained flat with a value around 1 for one decade, indicating that the capacitive current was equal to resistive current. Then in the third region, it decreased with frequency due to increased capacitive current. Network response followed the respective generator's responses.

8 DISCUSSION

The studies show that RVM and PCM studies can be used to study the fast and slow relaxation processes occurring in power equipment and network. Using the derived equations and RVM or PCM measured results, dielectric response function of each equipment and parameters to relate the aging characteristics for condition monitoring can be determined using extended Debye and universal fractional power law models. In RVM studies, all the measured RVM responses in different power apparatus showed a single peak response with the developed high impedance measurement system. The RVM response was linear with charging voltage, which enabled us to do modelling with a lumped electrical circuit or with a dielectric response function. With 100 V as a charging voltage and by keeping charging time to discharging time as 2, trans-

formers of a rating from 2.2 to 300 MVA aged about 16 to 18 years had a maximum recovery voltage in the order of 11.5 to 18.8 V. The tested cable of similar age and 300 MVA rating had a peak recovery voltage of 17.8 V and the two generators Ga1 and Gb1 had peaks at 2.2 V and 2.9 V respectively. When all apparatus were in the network, the peaks for network "SYS1" and "SYS2" were at 3.7 and 4.1 V, respectively. Time at peak voltage occurrence for transformers was in the range of 35 to 60 s, for the cable at 62 s, for generators in the range of 90 to 158 s and for the network system in the range of 77 to 98 s. By increasing $k = t_c/t_d$, a higher recovery voltage with fast rising response was obtained since the discharging time was reduced. In PCM studies, the measured current decreased monotonically with time and was linear with applied voltage. With energising voltage of 50 V, i_p at 1 s for transformers varied from 0.07 to 0.19 μA. i_p at 1 s for generators varied from 4.25 to 6.47 μA. i_p at 1 s for the cable was 0.52 μA. i_p at 1 s for systems varied from 4.76 to 4.92 μA. i_p at 1000 s for transformers varied from 0.02 to 0.04 μA. i_p at 1000 s for generators varied from 0.39 to 0.57 μA. i_p at 1000 s for the cable was 0.04 μA. i_p at 1000 s for systems varied from 0.44 to 0.69 μA.

To determine the parameters of remaining life indicators derived equations in section 2 on ED and UFPL models were used. In ED model, RVM responses fitted well and the difference between measured and predicted responses decreased with the increased number of relaxation elements. R_g and C_g converged to a finite value by increasing the number of polarizing elements. Evaluated time constants of relaxation elements varied from 0.2 to 2013 s for transformers, 0.4 to 35350 s for generators and 2 to 1430 s for the cable. The ED model parameters can be used to predict three existing aging indicators like: the maximum recovery voltage, time to reach the peak voltage and the initial slope. By fitting the ED model to individual RVM response with a "t_c" setting showed that the parameters may vary to a certain extent with variation in "t_c" setting and it can predict the measured results correctly. Studies in section 4.1.4 indicated that the fitted parameters on RVM response with each "t_c" fit differed from fit on all RVM responses. The cause of this error is to be identified either by taking more number of elements or by modifying the models or by replacing relaxation parameters as a function of time/frequency. In UFPL model, predicted dielectric response function shown in Figure 13 for generator was more linear with time than for transformers and the cable.

Normally an RVM measurement for an apparatus took about 10 h. PCM experimental results can be predicted with the ED model parameters extracted from RVM except for the 300 MVA generator. With UFPL model, the fitting was not good for both generators. It may be that relaxation in micaceous solid insulation should be studied more. A good correlation between RVM that investigated the recovery voltage across the test object produced by relaxation processes and PCM that studied the polarisation current through the test object can be established based on ED model. There are two methods to measure the different quantities controlled by the same underlying relaxation mechanism. In operational point of view, PCM was simpler and better than RVM since it took shorter time than RVM. From the analytical point of view to extract parameters, RVM was better than PCM since it was very difficult to extract parameters of the ED model accurately from one PCM response. Prediction of smaller network-"SYS1" RVM response using ED model parameters of individual apparatus was good except for $t_c = 1$ s. With larger network-"SYS2" RVM response, fitting was observed only for $t_c = 1$ s. Calculated recovery voltage was more in all the cases of "t_c" in "SYS2". This suggested that the injected charge might have found path locally. By optimizing R_g and C_g, a satisfactory fit shown in Figure 22 can be made for networks with ED model. In the prediction of low frequency response using ED model, the real part of admittance had three distinct regions in the frequency plane. The changeover occurred in the frequency band of 10^{-4} to 10^{-2} Hz. That frequency band corresponded to the relaxation band of the apparatus. The imaginary part of admittance had two distinct regions and in general, the variation increased linearly with frequency. The variation of dissipation factor had three distinct regions with resistive component dominating at the lowest frequency band. In the mid band, it remained constant around one. In the last band, the charging current due to capacitive element dominated.

9 CONCLUSION

STUDY on RVM and PCM in generating network indicated that these measurements could be used as quantitative condition monitoring tools for the determination of aging status of power apparatus. All RVM responses in different apparatus showed a single peak response with the developed high impedance measurement system. The response was linear with charging voltage in the range of 50 to 200 V_{dc}. A satisfactory RVM fitting can be made with ED model by taking 3 or more relaxation elements. PCM data also fitted well with ED model on transformers and cable but it did not fit well with generators. The relaxation model on solid insulation used in generators had to be improved. A better fitting could be achieved with the ED model in comparison to the UFPL model. The predicted dielectric relaxation spectrum $f(t)$ on generators was more linear in comparison with transformers and cable. The interrelationship between RVM and PCM was achieved in most of the apparatus. Network response can be predicted using ED model parameters of individual apparatus satisfactorily. The fitting parameters on individual curve response with a "t_c" setting on ED and UFPL models varied with all curves fitting and it suggested that the models have to be improved taking into

the effect of the parameter "t_c". Derived low frequency responses showed the range of relaxation spectrum for the aging apparatus.

ACKNOWLEDGMENT

The authors thank PowerSeraya Ltd. and PowerSenoko Ltd., Singapore for giving us the necessary facilities to conduct the relaxation studies on working equipment.

REFERENCES

[1] G. C. Montanari and D. K. Das-Gupta, "Polarization and Space Charge Behavior of Unaged and Electrically Aged Crosslinked Polyethylene", IEEE Trans. Dielectr. Electr. Insul., Vol. 7, pp. 474–479, 2000.

[2] J. M. Seifert, U. Stietzel and H. C. Karner, "The Ageing of Composite Insulating Materials—New Possibilities to Detect and to Classify Ageing Phenomena with Dielectric Diagnostic Tools", IEEE Int. Symp. Electr. Insul., Virginia, USA, pp. 373–377, 1998.

[3] N. H. Ahmed and N. N. Srinivas, "Review of Space Charge Measurement in Dielectrics", IEEE Trans. Dielectr. Electr. Insul., Vol. 4, pp. 644–656, 1997.

[4] A. G. Schlag, *The Recovery Voltage Method for Transformer Diagnosis*, Tettex Instruments, 1995.

[5] P. R. S. Jota, S. M. Islam and F. G. Jota, "Modeling the Polarization Spectrum in Composite Oil/paper Insulation Systems", IEEE Trans. Dielectric. Electr. Insul., Vol. 6, pp. 145-151, 1999.

[6] E. Ildstad, U. Gafvert and P. Tharning, "Relation Between Return Voltage and other Methods for Measurements of Dielectric Response", IEEE Int. Symp. Electr. Insul., pp. 25–28, 1994.

[7] T. K. Saha, and M. Darveniza, "Characterization of Thermally Accelerated Aged Oil-paper Transformer Insulation by Interfacial Polarization Spectra Measurements", 5th Int. Conf. Properties and Appl. Dielectric Materials, Vol. 1, pp. 463–466, 1997.

[8] R. Patsch and J. Jung, "Improvement of the Return Voltage Method for Water Tree Detection in XLPE Cables", IEEE Int. Symp. Electr. Insul., CA, USA, pp. 133–136, 2000.

[9] B. Jonuz, P. H. F. Morshuis, H. J. van Breen, J. Pellis and J. J. Smit, "Detection of Water Trees in Medium Voltage XLPE Cables by Return Voltage Measurements", IEEE Int. Symp. Electr. Insul., CA, USA, pp. 355–358, 2000.

[10] G. Csepes, I. Hamos, R. Brooks and V. Karius, "Practical Foundations of the RVM (Recovery Voltage Method for Oil/paper Insulation Diagnosis)", IEEE Conf. Electr. Insul. Dielectric Phenomena, Vol. 1, pp. 345–355, 1998.

[11] A. K. Jonscher, *Universal Relaxation Law*, Chelsea Dielectrics Press, London, 1996.

[12] A. Helgeson and U. Gafvert, "Dielectric Response Measurements in Time and Frequency Domain on High Voltage Insulation with Different Response", Int. Symp. Electr. Insul. Materials, pp. 393–398, 1998.

[13] *MATLAB Optimization Toolbox* user's guide, the Math Works, Inc., 1999.

[14] S. Amari and J. Bornemann, "Efficient Numerical Computation of Singular Integrals with Applications to Electromagnetics", IEEE Trans. Antennas and Propagation, Vol. 43, pp. 1343–1344, 1995.

[15] P. Osvath and H. Zahn, "Polarization Spectrum Analysis for Diagnosis of Oil/paper Insulation Systems", IEEE Int. Symp. Electr. Insul., pp. 155–161, 1994.

[16] J. P. Van Bolhuis, E. Gulski, J. J. Smit, G. M. Urbani and H. F. A. Verhaart, "Development of Knowledge Rules for RVM for Interpretation of the Condition of Transformer Insulation", IEEE Int. Symp. Electr. Insul., pp. 267–270, 2000.

[17] R Neimanis, T. K. Saha and R. Eriksson, "Determination of Moisture Content in Mass Impregnated Cable Insulation using Low Frequency Dielectric Spectroscopy", IEEE Int. Symp. Electr. Insul., pp. 463–468, 2000.

[18] V. Der Houhanessian and W. S. Zaengl, "Time Domain Measurements of Dielectric Response in Oil-paper Insulation Systems", IEEE Int. Symp. Electr. Insul., Vol. 1, pp. 47–52, 1996.

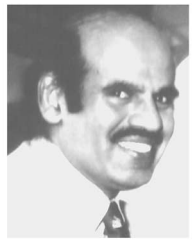

S. Birlasekaran (M'79-SM'99) received the M.E. with distinction in HV Engineering from IISc, Bangalore, India in 1970 and the Ph.D. in electrical engineering from the University of Queensland, Australia in 1980. He worked with CSIRO, Sydney, University of Newcastle and University of Bombay before moving to Nanyang Technological University, Singapore in 1998. He is an Associate Professor in Power Engineering. His research interests are condition monitoring of power apparatus and modeling of degradation process.

Yu Xingzhou received the M.Eng. degree from Nanyang Technological University in 2000. He is an Engineer working in the Condition Monitoring Division of PowerGrid Ltd., Singapore.